

Lattice damage in InGaN induced by swift heavy ion irradiation

Ning Liu(刘宁), Li-Min Zhang(张利民), Xue-Ting Liu(刘雪婷), Shuo Zhang(张硕), Tie-Shan Wang(王铁山), and Hong-Xia Guo(郭红霞)

Citation: Chin. Phys. B, 2022, 31 (**10**): 106103. DOI: 10.1088/1674-1056/ac7ccd
Journal homepage: http://cpb.iphy.ac.cn; http://iopscience.iop.org/cpb

What follows is a list of articles you may be interested in

Degradation of β-Ga_2O_3 Schottky barrier diode under swift heavy ion irradiation

Wen-Si Ai(艾文思), Jie Liu(刘杰), Qian Feng(冯倩), Peng-Fei Zhai(翟鹏飞), Pei-Pei Hu(胡培培), Jian Zeng(曾健), Sheng-Xia Zhang(张胜霞), Zong-Zhen Li(李宗臻), Li Liu(刘丽), Xiao-Yu Yan(闫晓宇), and You-Mei Sun(孙友梅)
Chin. Phys. B, 2021, 30 (**5**): 056110. DOI: 10.1088/1674-1056/abf107

Characterization of swift heavy ion tracks in MoS_2 by transmission electron microscopy

Li-Jun Xu(徐丽君), Peng-Fei Zhai(翟鹏飞)†, Sheng-Xia Zhang(张胜霞), Jian Zeng(曾健), Pei-Pei Hu(胡培培), Zong-Zhen Li(李宗臻), Li Liu(刘丽), You-Mei Sun(孙友梅), and Jie Liu(刘杰)‡
Chin. Phys. B, 2020, 29 (**10**): 106103. DOI: 10.1088/1674-1056/abad1e

Quasi-homoepitaxial GaN-based blue light emitting diode on thick GaN template

Li Jun-Ze, Tao Yue-Bin, Chen Zhi-Zhong, Jiang Xian-Zhe, Fu Xing-Xing, Jiang Shuang, Jiao Qian-Qian, Yu Tong-Jun, Zhang Guo-Yi
Chin. Phys. B, 2014, 23 (**1**): 016101. DOI: 10.1088/1674-1056/23/1/016101

Effect of $In_xGa_{1-x}N$ "continuously graded" buffer layer on InGaN epilayer grown by metalorganic chemical vapor deposition

Qian Wei-Ning, Su Shi-Chen, Chen Hong, Ma Zi-Guang, Zhu Ke-Bao, He Miao, Lu Ping-Yuan, Wang Geng, Lu Tai-Ping, Du Chun-Hua, Wang Qiao, Wu Wen-Bo, Zhang Wei-Wei
Chin. Phys. B, 2013, 22 (**10**): 106106. DOI: 10.1088/1674-1056/22/10/106106

Dual-blue light-emitting diode based on strain-compensated InGaN-AlGaN/GaN quantum wells

Yan Qi-Rong, Yan Qi-Ang, Shi Pei-Pei, Niu Qiao-Li, Li Shu-Ti, Zhang Yong
Chin. Phys. B, 2013, 22 (**2**): 026102. DOI: 10.1088/1674-1056/22/2/026102

Lattice damage in InGaN induced by swift heavy ion irradiation

Ning Liu(刘宁)[1,2], Li-Min Zhang(张利民)[2,†], Xue-Ting Liu(刘雪婷)[2], Shuo Zhang(张硕)[2], Tie-Shan Wang(王铁山)[2], and Hong-Xia Guo(郭红霞)[1]

[1] *State Key Laboratory of Laser Interaction with Matter, Northwest Institute of Nuclear Technology, Xi'an* 710024, *China*
[2] *School of Nuclear Science and Technology, Lanzhou University, Lanzhou* 730000, *China*

(Received 5 May 2022; revised manuscript received 24 June 2022; accepted manuscript online 29 June 2022)

The microstructural responses of $In_{0.32}Ga_{0.68}N$ and $In_{0.9}Ga_{0.1}N$ films to 2.25 GeV Xe ion irradiation have been investigated using x-ray diffraction, Raman scattering, ion channeling and transmission electron microscopy. It was found that the In-rich $In_{0.9}Ga_{0.1}N$ is more susceptible to irradiation than the Ga-rich $In_{0.32}Ga_{0.68}N$. Xe ion irradiation with a fluence of 7×10^{11} ions·cm^{-2} leads to little damage in $In_{0.32}Ga_{0.68}N$ but an obvious lattice expansion in $In_{0.9}Ga_{0.1}N$. The level of lattice disorder in $In_{0.9}Ga_{0.1}N$ increases after irradiation, due to the huge electronic energy deposition of the incident Xe ions. However, no Xe ion tracks were observed to be formed, which is attributed to the very high velocity of 2.25 GeV Xe ions. Point defects and/or small defect clusters are probably the dominant defect type in Xe-irradiated $In_{0.9}Ga_{0.1}N$.

Keywords: InGaN, swift heavy ions, irradiation effects

PACS: 61.80.–x, 78.66.Fd **DOI:** 10.1088/1674-1056/ac7ccd

1. Introduction

Indium gallium nitride (InGaN) is an important group III nitride semiconductor material. The bandgap of $In_xGa_{1-x}N$ can be tuned from 0.7 eV to 3.4 eV with decreasing In content x from 1 to 0,[1,2] which covers nearly the whole solar spectrum. Hence, InGaN has great potential for the development of multi-junction solar cells, light-emitting diodes (LEDs) and laser diodes (LDs).[3] One of the challenges for the application of InGaN materials is how to achieve p-type doping, in particular for In-rich $In_xGa_{1-x}N$ ($x>0.5$).[1] The ion implantation technique is widely used for ion doping in semiconducting materials.[4,5] As implantation-induced radiation damage is detrimental to effective doping, knowledge of the radiation effects in implanted materials is essential for the application of ion implantation. Over the past decade, extensive research effort has been devoted to radiation studies of InGaN.[6–12] It has been found that the resistance of InGaN to irradiation-induced amorphization dramatically decreases with increasing In concentration in InGaN. While GaN is fully amorphized by room-temperature irradiation of 1 MeV Au ions to a dose of $\sim$ 90 dpa (displacements per atom),[13] the amorphization dose for $In_{0.2}Ga_{0.8}N$ under a similar irradiation condition is only $\sim$ 1.4 dpa.[8] The lattice structure of $In_xGa_{1-x}N$ ($x\geq0.7$) irradiated with 5 MeV Xe ions at room temperature was observed to break down at doses of no more than 0.1 dpa.[9] The decreasing radiation resistance of the high In-content InGaN is primarily attributed to a smaller cohesive energy of the In–N bond, which results in a reduced dynamic annealing efficiency.[9] However, to date, little is known about the response of InGaN to irradiation with swift heavy ions (SHIs) with ion energies larger than several tens of MeV. Unlike the case of low-energy ion irradiation, huge electronic energy deposition is produced in materials by SHI irradiation. Ion tracks with a modified material structure along the ion incidence direction will be created when the electronic stopping power (S_e) of incident ions exceeds a certain threshold;[14] otherwise annealing of the pre-existing lattice defects probably occurs. SHIs with large projected ion ranges can be used for deep ion implantation of materials. In addition, the application of InGaN-based electronics in outer space will suffer from SHI irradiation. Hence it is important to understand the radiation effects of SHIs in InGaN. This work focuses on the dependence on In content of radiation hardness of InGaN to SHI irradiation. Both $In_{0.32}Ga_{0.68}N$ and $In_{0.9}Ga_{0.1}N$ films are irradiated with 2.25 GeV Xe ions and then characterized by high-resolution x-ray diffraction (HRXRD), Raman scattering, Rutherford backscattering spectrometry in channeling geometry (RBS/C) and transmission electron microscopy (TEM). The reported results will improve the current understanding of SHI irradiation-induced damage effects in InGaN, and may have important implications for the ion implantation and space electronics of InGaN materials.

2. Experiments

The wurtzite $In_xGa_{1-x}N$ films used in this work were grown by metal–organic chemical vapor deposition (MOCVD) on c-plane sapphire (Al_2O_3) substrates with 2 μm thick GaN interlayers. Based on the analysis of Rutherford backscattering spectrometry (RBS), the In content x in the two different $In_xGa_{1-x}N$ samples was determined to be

†Corresponding author. E-mail: zhanglm@lzu.edu.cn

© 2022 Chinese Physical Society and IOP Publishing Ltd

0.32 and 0.9 ± 0.01, respectively; the film thicknesses of the $In_{0.32}Ga_{0.68}N$ and $In_{0.9}Ga_{0.1}N$ were $\sim$ 290 nm and 350 nm. The samples were cut into 4 mm×4 mm squares for ion irradiation. SHI irradiation experiments were performed at the Heavy Ion Research Facility in Lanzhou in the Institute of Modern Physics, Chinese Academy of Sciences. The 2.52 GeV $^{129}Xe^{27+}$ ions were provided by the sector-focused cyclotron and sector-separated cyclotron. In order to count and decelerate the Xe ions, high-purity Al foils were placed in front of the samples with the foil surface normal to the incident ion beam. After penetrating the foils, the incident Xe ions are slowed down to an energy of 2.25 GeV according to the SRIM simulation,[15] and they are expected to attain charge-state equilibrium. The mean equilibrium charge state of 2.25 GeV Xe ions in solids is calculated by the CasP code to be 48^+.[16] The samples were then irradiated at room temperature and normal incidence to ion fluences of 3×10^{11} ions·cm^{-2} and 7×10^{11} ions·cm^{-2} with a beam flux of 3×10^8 ions·cm^{-2}·s^{-1}. The $In_{0.32}Ga_{0.68}N$ and $In_{0.9}Ga_{0.1}N$ samples were irradiated simultaneously by placing them side by side under a uniform beam spot. The incident Xe ions penetrate the InGaN films and underlying GaN interlayers completely and terminate in the Al_2O_3 substrates. For a comparison study, the $In_{0.9}Ga_{0.1}N$ sample was also irradiated at room temperature with 5 MeV $^{129}Xe^{20+}$ ions at the 320 kV platform for multidisciplinary research at the Institute of Modern Physics, Chinese Academic of Sciences. The irradiation was conducted at normal incidence to a fluence of 3×10^{11} ions·cm^{-2} with a beam flux of 1×10^{11} ions·cm^{-2}·s^{-1}. After irradiation, the samples were characterized by HRXRD using a Bruker D8 diffractometer. ω–2θ scans of the (0002) plane of the samples were performed in triple-axis mode with a Cu $K\alpha$ source. The angular resolution of the spectra was 0.005°. The Raman scattering measurements were carried out using a LabRAM HR 800UV spectrometer (Horiba Jobin-Yvon). In order to reduce the Raman signal from the GaN sublayers, the 325 nm line of a Cd–He laser was used as the excitation source. The laser beam was focused onto a spot with a diameter of $\sim$ 3 μm at the sample surface. The Raman spectral resolution was better than 1 cm^{-1}. The RBS/C measurements were performed with a 2 MeV He^+ ion beam incident along $\langle 0001 \rangle$ direction of the samples and recorded by a detector at a backscattering angle of 150° or 165°. The backscattering yields have an uncertainty of $\sim$ 7% due to the inaccuracy of current integration. Cross-sectional TEM foils with a thickness of $\sim$ 50 nm were prepared using a focused ion beam system after application of a protective Pt/Au layer on the sample surface. TEM was performed on the samples using FEI TF30 at an accelerating voltage of 300 kV.

3. Results

3.1. HRXRD results

Figure 1 illustrates the HRXRD spectra of the $In_{0.32}Ga_{0.68}N$ and $In_{0.9}Ga_{0.1}N$ (0002) peaks before and after 2.25 GeV Xe ion irradiation to a fluence of 7×10^{11} ions·cm^{-2}. It is seen that the intensities of the InGaN peaks are weak, because the InGaN films are thin and the sample sizes are very small. The full width at half maximum (FWHM) values of the virgin $In_{0.32}Ga_{0.68}N$ and $In_{0.9}Ga_{0.1}N$ are roughly estimated to be 0.14° and 0.06°, respectively. This suggests that the $In_{0.9}Ga_{0.1}N$ film has a better crystal quality than $In_{0.32}Ga_{0.68}N$. The analysis of the virgin (0002) peaks leads to lattice parameters of $c = 0.5386$ nm for $In_{0.32}Ga_{0.68}N$ and $c = 0.5704$ nm for $In_{0.9}Ga_{0.1}N$, respectively. Using Vegard's law,[17] the c_0 values of perfect $In_{0.32}Ga_{0.68}N$ and $In_{0.9}Ga_{0.1}N$ are estimated to be 0.5351 nm and 0.5651 nm, with the assumptions of $c_0 = 0.5186$ nm for GaN and $c_0 = 0.5703$ nm for InN. The virgin $In_{0.32}Ga_{0.68}N$ and $In_{0.9}Ga_{0.1}N$ exhibit slight lattice strains $[(c - c_0)/c_0 \times 100\%]$ of $\sim$ 0.6% and 0.9%, which originate from the differences in lattice constants and thermal expansion coefficients between the InGaN and GaN substrates.[1] After Xe ion irradiation, no significant changes in FWHM of the diffraction peaks are induced for either $In_{0.32}Ga_{0.68}N$ or $In_{0.9}Ga_{0.1}N$. The $In_{0.32}Ga_{0.68}N$ peak in Fig. 1(a) exhibits a slight shift of 0.01° towards higher angles with respect to the unirradiated peak.

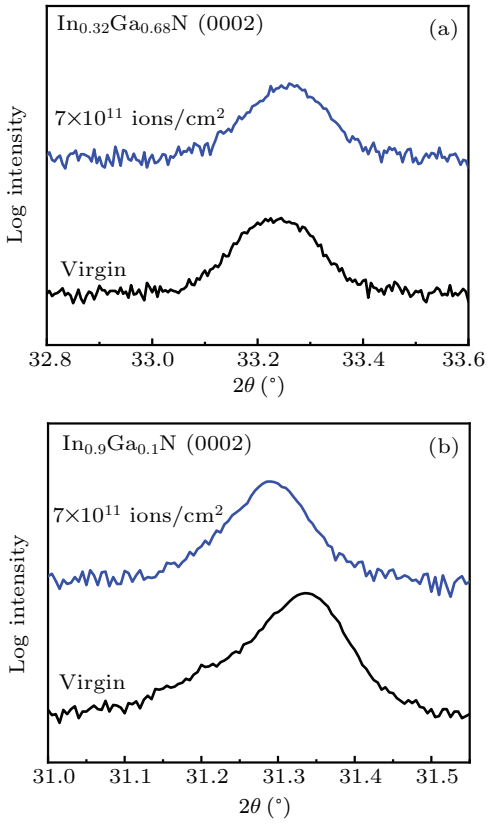


Fig. 1. HRXRD spectra for (a) $In_{0.32}Ga_{0.68}N$ and (b) $In_{0.9}Ga_{0.1}N$ films before and after 2.25 GeV Xe ion irradiation at room temperature to a fluence of 7×10^{11} ions·cm^{-2}.

Normally, ion irradiation causes lattice expansion in nitride materials, which results in a shift of the diffraction peaks towards lower angles.[18] The abnormal shift of the $In_{0.32}Ga_{0.68}N$ peak may be attributed to a slight compositional difference in those samples. The InGaN samples used in this work are cut from an InGaN wafer grown by MOCVD with a diameter of 2 inches. The In content and film thickness are different in different regions of the wafer. However, the differences are slight and cannot be resolved by RBS and Raman spectroscopy, as shown below. In contrast to $In_{0.32}Ga_{0.68}N$, the $In_{0.9}Ga_{0.1}N$ peak obviously shifts towards smaller angles. The shift indicates an irradiation-induced lattice expansion in $In_{0.9}Ga_{0.1}N$, which is ascribed to the accumulation of various point defects, which is common in nitride materials.[10,14] The corresponding lattice strain along the *c*-axis is increased to 1.1%. The XRD results suggest that, as in the case of low-energy heavy-ion irradiation,[9] the In-rich $In_{0.9}Ga_{0.1}N$ is more sensitive to SHI irradiation than the Ga-rich $In_{0.32}Ga_{0.68}N$.

3.2. Raman results

Figure 2 shows the Raman spectra for the $In_{0.32}Ga_{0.68}N$ and $In_{0.9}Ga_{0.1}N$ films before and after 2.25 GeV Xe ion irradiation to a fluence of 7×10^{11} ions·cm^{-2}. In addition to the E_2(high) and A_1(longitudinal optical, LO) peaks from the InGaN films, there are two fluorescence-induced background peaks at 323 cm^{-1} and 573 cm^{-1}. For $In_{0.32}Ga_{0.68}N$, there is a shoulder on the low-frequency side of the A_1(LO) peak, which is assigned as a disorder-activated E_1(LO) mode due to the poor crystal quality of $In_{0.32}Ga_{0.68}N$.[19] The intensity of the A_1(LO) peak from the $In_{0.9}Ga_{0.1}N$ film is very weak, which is attributed to the increasing electron carrier concentration in $In_{0.9}Ga_{0.1}N$ that damps the LO phonons via phonon–plasmon coupling.[20,21] After Xe ion irradiation, no changes are revealed in the Raman spectrum of $In_{0.32}Ga_{0.68}N$ whereas the E_2(high) peak of $In_{0.9}Ga_{0.1}N$ shifts from 497 cm^{-1} to 501 cm^{-1}, as shown in the inset of Fig. 2(b). The blue shift of the E_2(high) peak suggests the existence of a compressive stress in the irradiated $In_{0.9}Ga_{0.1}N$[22] associated with the irradiation-induced lattice expansion. This is in good agreement with the XRD observation in Fig. 1.

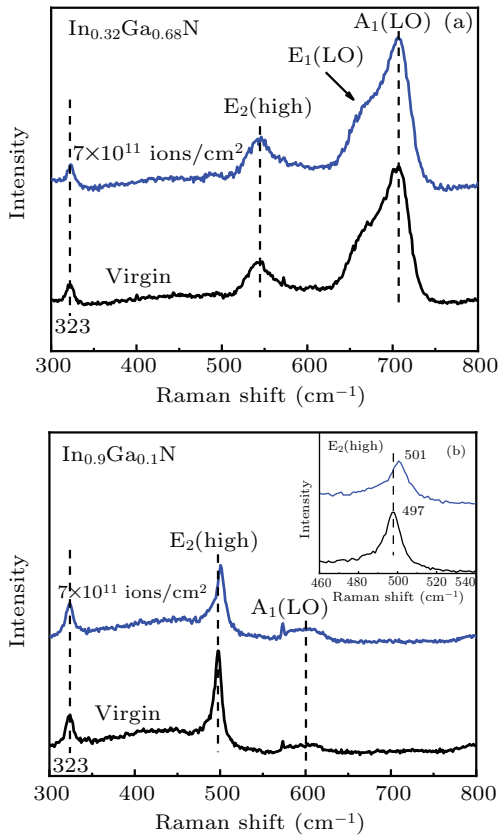


Fig. 2. Raman spectra for (a) $In_{0.32}Ga_{0.68}N$ and (b) $In_{0.9}Ga_{0.1}N$ films before and after 2.25 GeV Xe ion irradiation at room temperature to a fluence of 7×10^{11} ions·cm^{-2}. The inset shows the magnified E_2(high) peak from $In_{0.9}Ga_{0.1}N$.

3.3. RBS/C results

Figure 3 displays the RBS random and ⟨0001⟩-aligned channeling spectra for the $In_{0.32}Ga_{0.68}N$ and $In_{0.9}Ga_{0.1}N$ films on GaN before and after 2.25 GeV Xe ion irradiation to a fluence of 7×10^{11} ions·cm^{-2}. The depth scales of the In and Ga sublattices are obtained using the He stopping power from the SRIM database. The simulation results of random spectra using the SIMNRA 7.0 code[23] are also included in the figures, from which the film composition and thickness are estimated. For the virgin $In_{0.9}Ga_{0.1}N$, the minimum backscattering yield (χ_{min}) as determined by the yield ratio of the channeling to a random spectrum in the near-surface region is 4.7%, typical for a perfect crystal. By contrast, the χ_{min} for the virgin $In_{0.32}Ga_{0.68}N$ is as high as 47%, which is attributed to the large lattice mismatch between GaN and InN.[1] As shown in Fig. 3, Xe ion irradiation leads to little damage in $In_{0.32}Ga_{0.68}N$, as suggested by the RBS/C yields before and after irradiation. However, the $In_{0.9}Ga_{0.1}N$ is damaged under the identical irradiation condition, which is consistent with the HRXRD and Raman scattering results. The relative In disorder in the irradiated $In_{0.9}Ga_{0.1}N$, D_r, can be calculated from

$$D_r = (Y_{ic} - Y_{vc})/(Y_{vr} - Y_{vc}), \quad (1)$$

where Y_{vc} and Y_{vr} are the integrated yields of the channeling and random spectra from the virgin film and Y_{ic} is the integrated yield of the irradiated channeling spectrum. The backscattering yields are integrated in a small depth region from 50 nm to 75 nm just below the sample surface, where the influence of angular dispersion of the incident He ions on the RBS/C yields can be neglected. The D_r value of the Xe-irradiated $In_{0.9}Ga_{0.1}N$ film is calculated to be 5%.

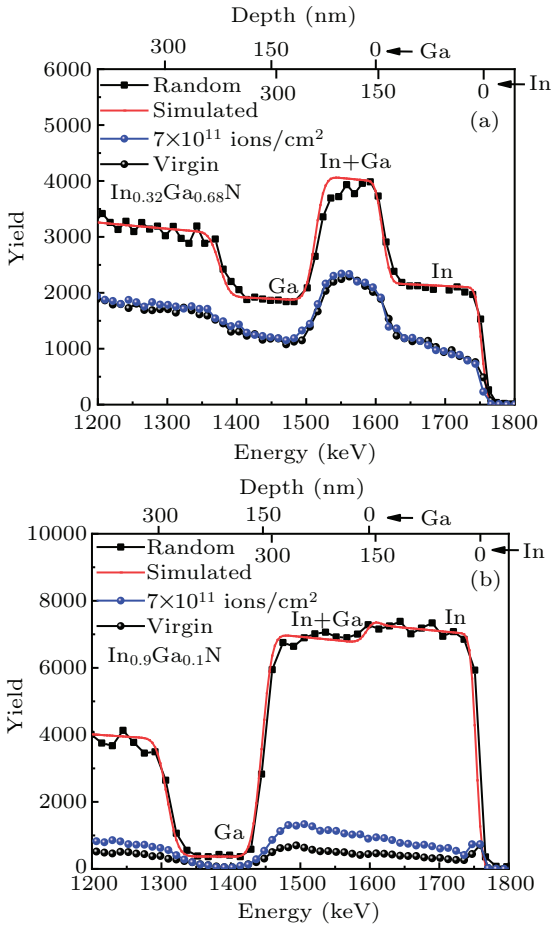


Fig. 3. RBS/C spectra together with the random spectra for (a) $In_{0.32}Ga_{0.68}N$ and (b) $In_{0.9}Ga_{0.1}N$ films grown on GaN before and after 2.25 GeV Xe ion irradiation to a fluence of 7×10^{11} ions·cm^{-2}. The red curves are simulation results of the random spectra using the SIMNRA code.

3.4. TEM results

In order to investigate whether 2.25 GeV Xe ion irradiation leads to the formation of ion tracks in $In_{0.9}Ga_{0.1}N$, the Xe-irradiated $In_{0.9}Ga_{0.1}N$ sample was characterized by cross-sectional TEM. The sample irradiated with an ion fluence of 3×10^{11} ions·cm^{-2} was used for the characterization, because overlapping of ion tracks probably occurs in the TEM image at a larger fluence.[24] The TEM image of the Xe-irradiated sample is shown in Fig. 4(a), together with the corresponding selected area electron diffraction pattern. Dislocation loops (black spots) as well as dislocation lines that penetrate the $In_{0.9}Ga_{0.1}N$ film along the film growth direction are observed. These dislocations also exist in the pristine $In_{0.9}Ga_{0.1}N$ (data not shown), implying that they are formed during the epitaxial growth of the $In_{0.9}Ga_{0.1}N$ film, which is common for nitride films.[25,26] Figure 4(b) shows the high-resolution TEM image of the Xe-irradiated $In_{0.9}Ga_{0.1}N$ together with the corresponding fast-Fourier transform pattern. The $In_{0.9}Ga_{0.1}N$ exhibits an intact lattice structure after irradiation. Assuming that highly disordered or amorphous ion tracks are formed in $In_{0.9}Ga_{0.1}N$, the track diameter should be ~ 3 nm (estimated from the RBS/C spectra). The detailed calculation method can be found in Ref. [14]. However, no such ion tracks are revealed in the TEM image. This suggests that point defects and/or small defect clusters are probably the dominant defect types in the Xe-irradiated $In_{0.9}Ga_{0.1}N$, and these cannot be resolved by conventional TEM. Instead, XRD, Raman scattering and RBS/C are very sensitive to these defects.

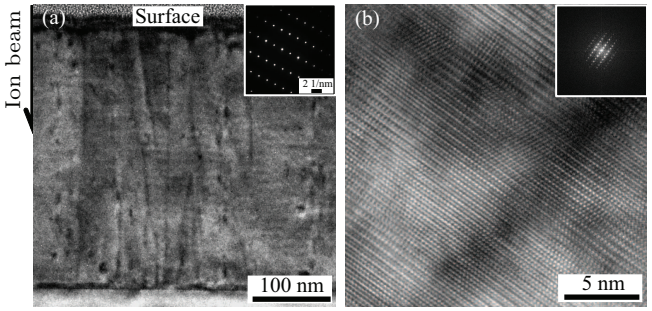


Fig. 4. (a) Cross-sectional TEM image and corresponding selected area electron diffraction pattern and (b) high-resolution TEM image and corresponding fast Fourier transform pattern of $In_{0.9}Ga_{0.1}N$ irradiated with 2.25 GeV Xe ions to a fluence of 3×10^{11} ions·cm^{-2}.

4. Discussion

In the present study, $In_{0.9}Ga_{0.1}N$ is found to be more sensitive to 2.25 GeV Xe ion irradiation than $In_{0.32}Ga_{0.68}N$. This agrees well with our previous irradiation study of $In_xGa_{1-x}N$ ($x = 0.32$–1.0) using 5 MeV Xe ions, which shows that the radiation resistance of InGaN decreases with increasing In concentration.[9] The decreasing radiation resistance of In-rich InGaN is mainly attributed to the smaller cohesion energy of the In–N bond (7.970 versus 9.058 eV/atom for the Ga–N bond). As a consequence, the broken In–N bonds are more difficult to restore than Ga–N bonds, which reduces the dynamic annealing efficiency in In-rich InGaN. In addition, the formation enthalpy of InGaN decreases with increasing In concentration, which leads to a decrease in the intrinsic stability of In-rich InGaN.[9] However, unlike the case of 5 MeV Xe ion irradiation, 2.25 GeV Xe ion irradiation creates lattice damage in $In_{0.9}Ga_{0.1}N$, primarily via intense electronic excitation rather than ballistic collision. For comparison, the $In_{0.9}Ga_{0.1}N$ sample irradiated with 5 MeV Xe ions at room temperature to a fluence of 3×10^{11} ions·cm^{-2} was characterized by RBS/C, and the results are shown in Fig. 5. According to the SRIM calculation, the projected range of 5 MeV Xe ions in the InGaN/GaN samples is ~ 1.1 μm, which is about four times greater than the thickness of the $In_{0.9}Ga_{0.1}N$ film. Hence, the incident Xe ions penetrate the $In_{0.9}Ga_{0.1}N$ film and create a nearly homogeneous damage distribution in the film. It is seen from Fig. 5 that 5 MeV Xe ion irradiation leads to little increase in RBS/C yields. The D_r value estimated from the near-surface region of the film is only 1.7%, which is lower than the value of 5% induced by 2.25 GeV Xe ion irradiation at 7×10^{11} ions·cm^{-2}. The corresponding SRIM-calculated displacement damage dose at the near-

surface region is 6×10^{-4} dpa for 5 MeV Xe irradiation of 3×10^{11} ions·cm^{-2}, but only 1.3×10^{-5} dpa for 2.25 GeV Xe irradiation of 7×10^{11} ions·cm^{-2}. This means that 2.25 GeV Xe ion irradiation leads to a higher lattice disorder with a much lower displacement damage dose. Obviously, the huge electronic energy deposition accounts for the damage production in $In_{0.9}Ga_{0.1}N$ irradiated with 2.25 GeV Xe ions. According to the thermal spike model,[27–31] target electrons are excited as a result of extremely high electronic energy deposition under SHI irradiation. The excited electrons transfer their energy to lattice atoms via electron–phonon coupling in a few picoseconds. This strong coupling effect between electronic and atomic subsystems can result in the formation of atomic-level defects.[32]

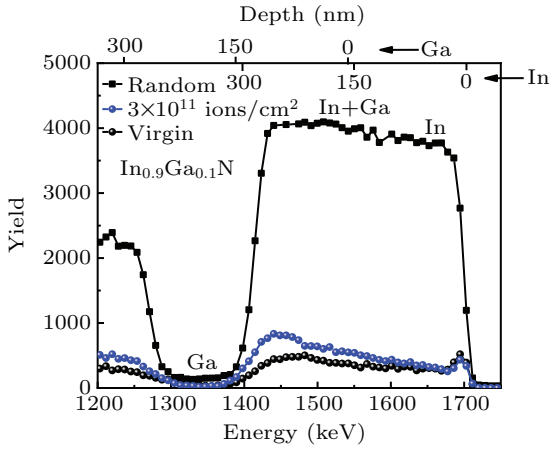


Fig. 5. RBS/C spectra together with the random spectra for $In_{0.9}Ga_{0.1}N$ films on GaN/Al_2O_3 before and after 5 MeV Xe ion irradiation at room temperature to a fluence of 3×10^{11} ions·cm^{-2}.

Although 2.25 GeV Xe ion irradiation produces lattice damage in $In_{0.9}Ga_{0.1}N$, no ion tracks are observed to be formed. It was found that the S_e threshold for ion track formation in GaN is between 22.8 keV·nm^{-1} and 28.3 keV·nm^{-1}.[33] InGaN and InN were found to be more susceptible to SHI irradiation than GaN.[9,14] For InN, ion tracks of 3.6 nm in diameter are created by 104 MeV Pb ions with a S_e value of 22 keV·nm^{-1}.[30] The S_e value of 2.25 GeV Xe ions in $In_{0.9}Ga_{0.1}N$ is calculated by SRIM to be 23 keV·nm^{-1}. The absence of ion tracks in Xe-irradiated $In_{0.9}Ga_{0.1}N$ could be attributed to the very high velocity of the Xe ions. For SHIs in solids, the higher the ion velocity, the larger the volume in which the electronic energy is deposited (the so-called velocity effect).[34–36] As a result, ion tracks are more likely to be formed for SHIs with a lower velocity because of the larger electronic energy deposition density. Using the inelastic thermal spike model,[30] the S_e thresholds for the formation of ion tracks in InN and GaN were predicted to increase with increasing ion velocity from 0.5 MeV·u^{-1} to 4.5 MeV·u^{-1}. Since the velocity of 2.25 Xe ions is as high as 17 MeV·u^{-1}, the electronic energy deposition density of the Xe ions in $In_{0.9}Ga_{0.1}N$ could be too low to induce ion tracks. Point defects and defect clusters are therefore expected to be the dominant defect type in the Xe-irradiated $In_{0.9}Ga_{0.1}N$.

5. Conclusions

Wurtzite $In_{0.32}Ga_{0.68}N$ and $In_{0.9}Ga_{0.1}N$ films were irradiated with 2.25 GeV Xe ions to 3×10^{11} ions·cm^{-2} and 7×10^{11} ions·cm^{-2} at room temperature. The irradiated films were analyzed by HRXRD, Raman scattering, RBS/C and TEM. The radiation resistance of $In_xGa_{1-x}N$ was found to decrease with increasing In content x. The HRXRD and Raman scattering results show that Xe ion irradiation leads to lattice expansion along with lattice strain in $In_{0.9}Ga_{0.1}N$. By contrast, there are almost no structural changes in $In_{0.32}Ga_{0.68}N$ under identical radiation conditions. The level of lattice disorder, as determined by RBS/C, increases in $In_{0.9}Ga_{0.1}N$ after irradiation. The intense electronic excitation rather than ballistic collision is confirmed to account for the production of damage. However, no ion tracks were observed in the TEM images of Xe-irradiated $In_{0.9}Ga_{0.1}N$, which is due to the velocity effect of SHIs in solids. Point defects and/or small defect clusters are probably the main radiation damage in $In_{0.9}Ga_{0.1}N$, and these cannot be resolved by conventional TEM but are very sensitive to XRD, Raman scattering and RBS/C.

Acknowledgements

The authors thank the staff of the Heavy Ion Research Facility in Lanzhou and the 320 kV platform in the Institute of Modern Physics, Chinese Academy of Sciences for support with the ion irradiation. We are grateful to Professor R. C. Fadanelli at the Federal University of Rio Grande do Sul, Brazil for his kind help with the RBS/C measurements.

Project supported by the National Natural Science Foundation of China (Grant No. 11875154) and State Key Laboratory of Intense Pulsed Radiation Simulation and Effect (Grant No. SKLIPR2014).

References

[1] Mclaughlin D V P and Pearce J M 2013 *Metall. Mater. Trans. A* **44A** 1947
[2] Wu J, Walukiewicz W, Yu K M, Shan W, Ager III J W, Haller E E, Lu H, Schaff W J, Metzger W K and Kurtz S 2003 *J. Appl. Phys.* **94** 6477
[3] Qu S D, Xu M S, Wang C X, Shi K J, Li R, Wei Y H, Xu X G and Ji Z W 2022 *Chin. Phys. B* **31** 017801
[4] Meng K, Jiang S L, Hou L N, Li C, Wang K, Ding Z B and Yao S D 2006 *Acta Phys. Sin.* **55** 2476 (in Chinese)
[5] Yao S D, Zhou S Q, Yang Z J, Lu Y H, Sun C C, Sun C, Zhang G Y, Vantomme A, Pipeleers B and Zhao Q 2003 *Chin. Phys. Lett.* **20** 102
[6] Kucheyev S O, Williams J S, Zou J, Pearton S J and Nakagawa Y 2001 *Appl. Phys. Lett.* **79** 602
[7] Wendler E, Wesch W, Alves E and Kamarou A 2004 *Nucl. Instrum. Methods. Phys. Res. B* **218** 36
[8] Kucheyev S O, Williams J S, Zou J and Jagadish C 2004 *J. Appl. Phys.* **95** 3048
[9] Zhang L M, Jiang W L, Dissanayake A, Peng J X, Ai W S, Zhang J D, Zhu Z H, Wang T S and Shutthanandan V 2016 *J. Appl. Phys.* **119** 245704

[10] Zhang L M, Fadanelli R C, Hu P, Zhao J T, Wang T S and Zhang C H 2015 *Nucl. Instrum. Methods. Phys. Res. B* **356** 53

[11] Zhang L M, Zhang C H, Zhang L Q, Jia X J, Han L H, Xu C L, Zhang Y and Jin Y F 2011 *Nucl. Instrum. Methods. Phys. Res. B* **269** 1063

[12] Zhang S, Wang B W, Zhang L M, Liu N, Wang T S, Duan B H and Xu X G 2021 *J. Phys. D: Appl. Phys* **54** 245104

[13] Jiang W, Weber W J, Wang L M and Sun K 2004 *Nucl. Instrum. Methods. Phys. Res. B* **218** 427

[14] Zhang L M, Jiang W, Fadanelli R C, Ai W S, Peng J X, Wang T S and Zhang C H 2016 *Nucl. Instrum. Methods. Phys. Res. B* **388** 30

[15] Ziegler J F, Biersack J P and Littmark U 2008 SRIM version

[16] Schiwietz G and Grande P L 2011 CasP v.6.0

[17] Yam F K and Hassan Z 2008 *Super. Microst.* **43** 1

[18] Gou J, Zhang L Q, Zhang C H, Song Y, Yang YT, Li J J, Meng Y C and Li H X 2013 *Nucl. Instrum. Methods. Phys. Res. B* **307** 89

[19] Ai W S, Zhang L M, Jiang W, Peng J X Chen L and Wang T S 2018 *Nucl. Instrum. Methods. Phys. Res. B* **415** 48

[20] Zolper J C, Pearton S J, Abernathy C R and Vartuli C B 1995 *Appl. Phys. Lett.* **66** 3042

[21] Alexson D, Bergman L, Nemanich R J, Dutta M, Stroscio M A, Parker C A, Bedair S M, El-Masry N A and Adar F 2001 *J. Appl. Phys.* **89** 798

[22] Park B G, Kumar R S, Moon M L, Kim M D, Kang T W, Yang W C and Kim S G 2015 *Jour. Cryst. Growth* **425** 149

[23] Mayer M, SIMNRA v.7.0, https://mam.home.ipp.mpg.de

[24] Hu P P, Liu J, Zhang S X, Maaz K, Zeng J, Guo H, Zhai P F, Duan J L, Sun Y M and Hou M D 2016 *Nucl. Instrum. Methods. Phys. Res. B* **372** 29

[25] Liliental-Weber Z, Jones R E, van Genuchten H C M, Yu K M, Walukiewicz W, Ager III J W, Haller E E, Lu H and Schaff W J 2007 *Physica B* **401** 646

[26] Liliental-Weber Z, Zakharov D N, Yu K M, Ager III J W, Walukiewicz W, Haller E E, Lu H and Schaff W J 2005 *J. Electron Microsc* **54** 243

[27] Kamarou A, Wesch W, Wendler E, Undisz A and Rettenmayr M 2006 *Phys. Rev. B* **73** 184107

[28] Schnohr C S, Kluth P, Giulian R and Llewellyn D J 2010 *Phys. Rev. B* **81** 075201

[29] Toulemonde M, Dufour C and Paumier E 1992 *Phys. Rev. B* **46** 14362

[30] Sall M, Monnet I, Moisy F, Grygiel C, Jublot-Leclerc S, Della-Negra S, Toulemonde M and Balanzat E 2015 *J. Mater. Sci* **50** 5214

[31] Xu L J, Zhai P F, Zhang S X, Zeng J, Hu P P, Li Z Z, L L, Sun Y M and Liu J 2020 *Chin. Phy. B* **29** 106103

[32] Zhang Y and Weber W J 2020 *Appl. Phys. Rev.* **7** 041307

[33] Karlušić M, Kozubek R, Lebius H, Ban-d'Etat B, Wilhelm R A, Buljan M, Siketić Z, Scholz F, Meisch T, Jakšić M, Bernstorff S, Schleberger M and Šantić B 2015 *J. Phys. D: Appl. Phys* **48** 325304

[34] Meftah A, Brisard F, Costantini J M, Hage-Ali M, Stoquert J P, Studer F and Toulemonde M 1993 *Phys. Rev. B.* **48** 920

[35] Szenes G 1995 *Phys. Rev. B* **52** 6154

[36] Waligórski M P R, Hamm R N and Katz R 1986 *Nucl. Tracks Radiat. Meas.* **11** 309